Ligand Binding to Heme Proteins: Relevance of Low-Temperature Data†

Anjum Ansari, Ernesto E. DiIorio,‡ Dana D. Dlott,§ Hans Frauenfelder,* Icko E. T. Iben, Peter Langer,‖ Heinrich Roder,⊥ Todd B. Sauke, and Erramilli Shyamsunder

Department of Physics, University of Illinois at Urbana-Champaign, Urbana, Illinois 61801

Received July 9, 1985; Revised Manuscript Received February 10, 1986

ABSTRACT: Binding of carbon monoxide to the β chain of adult human hemoglobin has been studied by flash photolysis over the time range from about 100 ps to seconds and the temperature range from 40 to 300 K. Below about 180 K, binding occurs directly from the pocket (process I) and is nonexponential in time. Above about 180 K, some carbon monoxide molecules escape from the pocket into the protein matrix. Above about 240 K, escape into the solvent becomes measurable. Process I can be observed up to 300 K. The low-temperature data extrapolate smoothly to 300 K, proving that the results obtained below 180 K provide functionally relevant information. The experiments show again that the binding process even at physiological temperatures is regulated by the final binding step at the heme iron and that measurements at high temperatures are not sufficient to fully understand the association process.

The binding of dioxygen and carbon monoxide to heme proteins has been studied by many groups, both experimentally (Gibson, 1956; Antonini & Brunori, 1971; Austin et al., 1975; Alberding et al., 1978; Alpert et al., 1979; Dudell et al., 1979; Beece et al., 1980; Chernoff et al., 1980; Dudell et al., 1980; Friedman & Lyons, 1980; Lindqvist et al., 1981; Doster et al., 1982; Dlott et al., 1983; Henry et al., 1983) and theoretically (Hänggi, 1978; Case & Karplus, 1979; Agmon & Hopfield, 1983a,b; Young & Bowne, 1984). Many of the experiments quoted above have only been performed in a small range of temperature. Such limited data are not sufficient to develop a model that describes all features in a consistent way. In our own work we explored the binding process over a wide range in temperature (2–300 K) and time (30 ps to kiloseconds) and constructed a model that is consistent with the data in the entire temperature and time domain. However, a number of specific questions are still unsolved. One problem, in particular, has been stated by Henry and collaborators: "This comparison points to the need for further experiments to demonstrate the correspondence between the ligand rebinding processes observed at high and low temperatures" (Henry et al., 1983). In the present paper we address this issue, the relevance of low-temperature experiments and the validity of the extrapolation to high temperatures. The experimental results verify the validity of the extrapolation and demonstrate that low-temperature data are relevant for the understanding of function.

Model, Assumptions, and Questions

We have shown in a series of papers (Austin et al., 1975; Beece et al., 1980, Doster et al., 1982) that the photodissociation and binding of a small ligand to a heme protein can be described by

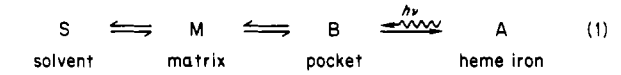

(1)

Here a ligand coming from the solvent (S) migrates through the protein matrix (M) to the heme pocket (B) and overcomes a final barrier at the heme to bind covalently to the heme iron (A). In a flash photolysis experiment, the system starts in well A in which the ligand is bound to the heme iron, for example, β^ACO.[1] The laser flash breaks the iron–CO bond, and the system rapidly moves to well B, where the CO molecule is in the heme pocket. At temperatures below about 180 K, the ligand cannot escape from the pocket and rebinds directly. We call the geminate recombination from the pocket *process I*. Figure 1 shows process I for the binding of CO to β^A, the isolated β chain of adult human hemoglobin. $\Delta A(t)$ is the observed change in absorbance as a function of time after photodissociation and is proportional to $N(t)$, the fraction of proteins that have not rebound a CO at the time t after photodissociation. The maximum change in absorbance, corresponding to complete photodissociation, is given by $\Delta A = 0.56$ OD. The values of ΔA shown in Figures 1 and 3–5 must be multiplied by 1.8 to obtain $N(t)$. As Figure 1 shows,

† This work was supported in part by the U.S. Department of Health and Human Services under Grant GM18051 and the National Science Foundation under Grant DMB 82-09616. This work was also supported in part by the National Science Foundation, Solid State Chemistry under Grant DMR-84-15070 (to D.D.D.). E.E.D.I. kindly acknowledges an EMBO short-term fellowship. D.D.D. acknowledges a fellowship from the Alfred P. Sloan Foundation. P.L. acknowledges a fellowship from the North Atlantic Treaty Organization Science Council through the Deutscher Akademischer Austauschdienst.

* Author to whom correspondence should be addressed.

‡ Present address: Laboratorium für Biochemie I, ETH, Zürich, Switzerland.

§ Permanent address: Department of Chemistry, University of Illinois at Urbana–Champaign, Urbana, IL 61801.

‖ Present address: Max Planck Institute for Biophysics, Frankfurt, West Germany.

⊥ Present address: Department of Biochemistry and Biophysics, University of Pennsylvania School of Medicine, Philadelphia, PA 19104.

[1] Abbreviations: Hb, human hemoglobin; Hb^A, adult human hemoglobin; Hb^{ZH}, abnormal human hemoglobin Zürich; β^A, separated β chains of human hemoglobin; β^{ZH}, separated β chains of hemoglobin Zürich; Mb, sperm whale myoglobin; CO, carbon monoxide; FTIR, Fourier transform infrared spectroscopy; EGOH, ethylene glycol. Processes I, M, and S are defined in the text, along with wells A, B, M, and S. $N(t)$ denotes the fraction of proteins that have not rebound a ligand at the time t after photodissociation. N_I denotes the fraction of photodissociated proteins that rebind the ligand via process I. Similarly, N_M and N_S are the amplitudes of process M and S, respectively. H_{BA} is the enthalpy of the barrier that is crossed in the rebinding step B → A (in kJ/mol). A_{BA} is the corresponding preexponential (in s^{-1}). k_{ij} is the rate coefficient for going from well i to well j, where wells i and j can be A, B, M, or S. λ_{on} is the pseudo-first-order rate coefficient characterizing the exponential solvent process. P_B is the occupation factor of well B. $g(H_{BA})$ is the fraction of proteins with the B → A barrier height in the range H_{BA} to $H_{BA} + dH_{BA}$. H_{BA}^{peak} is the barrier height at which the distribution $g(H_{BA})$ has a maximum value.

0006-2960/86/0425-3139$01.50/0

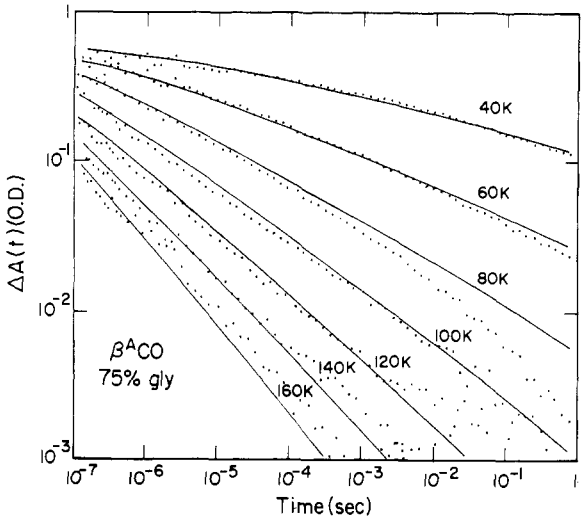

FIGURE 1: Recombination of CO with β^A in 75% (v/v) glycerol–water mixture buffered at pH 7.0, over the temperature range 40–160 K. $\Delta A(t)$ is the observed change in absorbance at the monitoring wavelength (436 nm), at time t after photodissociation. $\Delta A(t)$ is proportional to $N(t)$, the fraction of protein molecules that have not rebound CO at time t after photodissociation. $\Delta A(0)$ = 0.56 OD corresponds to $N(t)$ = 1. The solid lines are fits based on eq 3 by using the enthalpy distribution in Figure 2 and the preexponential factor in Table I.

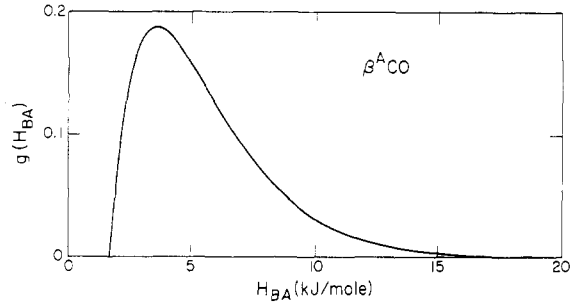

FIGURE 2: Activation enthalpy spectrum of the innermost barrier (H_{BA}) for β^A CO. The spectrum peaks at H_{BA}^{peak} = 3.6 kJ/mol.

process I is not exponential in time but can be approximated by a power law (Austin et al., 1975):

$$N(t) = (1 + t/t_0)^{-n} \quad (2)$$

where t_0 and n are temperature-dependent parameters. We explain the nonexponential time dependence by postulating that there is a distribution of barrier heights, $g(H_{BA})$, over the ensemble of protein molecules. $N(t)$ can then be expressed as

$$N(t) = \int_0^\infty dH_{BA} g(H_{BA}) \exp[-k_{BA}(H_{BA},T)t] \quad (3)$$

Above about 40 K, the rate coefficient k_{BA} for the step B → A is given by an Arrhenius relation:

$$k_{BA}(H_{BA},T) = A_{BA} \exp[-H_{BA}/(RT)] \quad (4)$$

From $N(t)$ measured between 40 and 160 K, $g(H_{BA})$ can be deduced (Austin et al., 1975). We have determined $g(H_{BA})$ and A_{BA} with increasing sophistication (Alberding et al., 1978; Dlott et al., 1983). The latest fit on the basis of the model of Young and Bowne (1984), drawn as solid lines in Figure 1, yields the distribution shown in Figure 2. The fit gives a preexponential $A_{BA} = (3.0 \pm 0.5) \times 10^9$ s^{-1} and a peak value for the distribution at $H_{BA}^{peak} = 3.6 \pm 0.2$ kJ/mol. H_{BA}^{peak} and A_{BA} depend only weakly on the choice of parametrization. The earlier techniques yield very similar values. We use here the form of $g(H_{BA})$ suggested by Young and Bowne because it

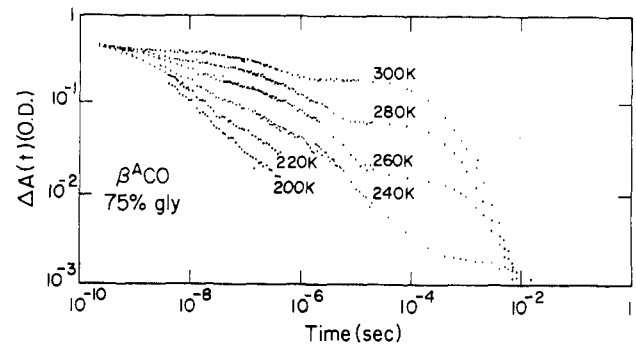

FIGURE 3: Rebinding of CO to β^A in 75% glycerol–water at 200–300 K. The solvent process becomes observable at 240 K.

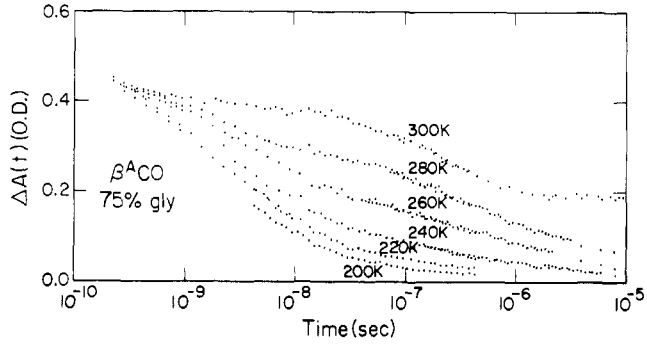

FIGURE 4: Expanded plot of the data in Figure 3. A linear $N(t)$ vs. log time plot emphasizes the break between I and M particularly at 280 and 300 K.

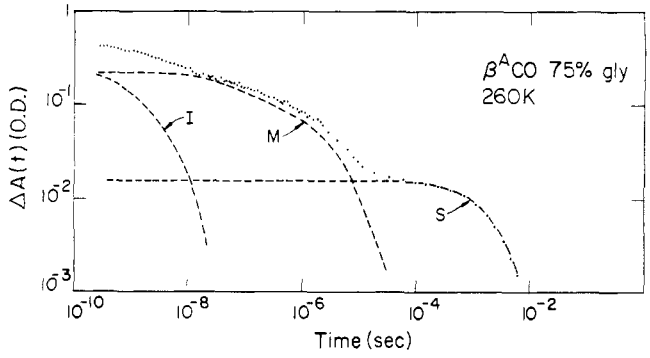

FIGURE 5: Decomposition of the recombination kinetics at 260 K into processes I, M, and S.

gives the best fit to the experimental data.

At temperatures above 180 K, the rebinding kinetics after photodissociation become more complex as is shown in Figures 3 and 4. $N(t)$ can be decomposed into three components, as done in Figure 5 (Dlott et al., 1983). In our model the three components have a straightforward explanation. The fastest component, process I, still corresponds to the direct rebinding from the heme pocket. A fraction of the ligands leave the pocket and escape into the protein matrix and eventually into the solvent. Process M is interpreted as the geminate recombination from the matrix or hydration shell. The solvent process S is a CO-concentration-dependent, nongeminate recombination process characterized by a pseudo-first-order rate coefficient λ_{on}.

In a rigid protein, a CO molecule in the pocket could not pass through the matrix into the solvent (Perutz & Matthews 1966; Case & Karplus 1979). In order for matrix and solvent processes to take place, the protein must fluctuate. Recently (Frauenfelder, 1985; Ansari et al., 1985) we have classified internal protein fluctuations. In Mb, and presumably also in β^A, four tiers of protein motions can be distinguished. Only

relaxation of tier I, which occurs above about 200 K, measurably affects the distribution of barrier heights $g(H_{BA})$. The distribution and the temperature dependence of the relaxation are not yet well-known, and consequently, we characterize it by an average relaxation rate $\bar{\lambda}_r$. At temperatures well below 200 K, $\bar{\lambda}_r$ is small compared to rebinding rates, each protein is frozen into a particular substate with a corresponding barrier height H_{BA}, and rebinding is nonexponential in time. At high temperatures $\bar{\lambda}_r$ becomes large compared to λ_{on} and a protein molecule will change its conformation rapidly on the time scale of the solvent process. The relevant theory has been treated in an earlier paper (Austin et al., 1975) with the central result that rebinding from the solvent becomes exponential in time if $\bar{\lambda}_r \gg \lambda_{on}$ (and if [CO] $\gg$ [Mb]). In this limit λ_{on} can be written as (Doster et al., 1982; Young, 1984)[2]

$$\lambda_{on}(T) = \bar{k}_{BA}(T)P_B(T)N_S(T) \quad (5)$$

with

$$\bar{k}_{BA}(T) = \int dH_{BA} g(H_{BA},T)k_{BA}(H_{BA},T) \quad (6)$$

Here $\bar{k}_{BA}(T)$ is the average rate coefficient for the step B $\rightarrow$ A. $P_B(T)$ is an occupation factor which, in the limit $k_{BA} \rightarrow 0$, is the probability of finding the system in well B. $N_S(T)$ is the fraction of systems initially in well B that move to well S, and $g(H_{BA},T)$ is determined from the low-temperature $g(H_{BA})$ either by assuming temperature independence of $g(H_{BA})$ throughout the entire temperature range (Austin et al., 1975) or by using a model, for instance that of Young and Bowne (1984). Equations 1–6 provide a consistent description of ligand binding. Establishing their validity is consequently important. Equations 4–6 rest on four assumptions (Dlott et al., 1983): (i) The sequential reaction eq 1 describes binding and photodissociation. The path through the matrix (M), however, can be complex and may involve many sequential and parallel pathways, some of which may be dead-ends. (ii) The covalent binding step, B $\rightarrow$ A, is present at high temperatures; regardless of the path through the globin, a ligand can only bind by overcoming the final barrier at the heme. (iii) Computation of the rate coefficient $\bar{k}_{BA}$ with eq 4 and 6 is a good approximation even at high temperatures. (iv) At high temperatures protein relaxation is fast compared to ligand association ($\bar{\lambda}_r \gg \lambda_{on}$).

We have justified assumptions i, ii, and iv in earlier papers, and we summarize the main arguments under Results and Discussion. Assumption iii, however, has been questioned. Henry et al. (1983), for instance, suggest that the final binding step could be much slower than predicted by eq 6. In the binding of CO to the isolated β chain from hemoglobin Zürich, the rate for process I levels off at about 200 K rather than increases as expected (Dlott et al., 1983). In the present work we explore the binding of CO to β^A in the time range from about 100 ps to 1 s and the temperature range from 40 to 300 K and show that assumption iii is correct for β^A. In addition, we have extended the studies of β^{ZH} to the picosecond regime and find a faster component of process I that is consistent with assumption iii. The slow component of process I in β^{ZH} can be due to the specific structure of β^{ZH}, which differs from β^A by the replacement of the distal histidine (E7) by an arginine. The replacement leads to an opening of the heme pocket to the solvent, and ligand dissociation induces drastic conformational changes on the distal side (Tucker et al., 1978; Phillips et al., 1981). In β^A the heme pocket is not open to the solvent, and it is therefore more suitable for testing assumption iii.

[2] In earlier papers, we have denoted N_S by N_{out}.

Materials and Methods

Isolated β^A and β^{ZH} chains were prepared in the carbonyl form under 1 atm of CO as described elsewhere (Giacometti et al., 1980; Doster et al., 1982). The samples were stored in liquid nitrogen until immediately before use.

Flash photolysis measurements in the nanosecond to second range were performed as previously described (Doster et al., 1982; Dlott et al., 1983). For the picosecond studies we used the pulse–probe method where a 75-ps pulse from a frequency-doubled Nd:YAG laser was split into two, with an intensity ratio 20:1. The stronger pulse photolyzed the sample while the weaker pulse served as the probe. The probe pulse was delayed with a corner-cube reflector on a motorized 160-cm delay line that provided up to 10.2 ns of delay. The relative delay was adjusted so that the probe pulse sampled before, during, and after photolysis. The signal from the photodiode was detected with a lock-in amplifier operating at the laser repetition rate of 200 Hz. The probe signals were averaged over about 50 sweeps of the delay line with a computer.

Results and Discussion

The experimental results are summarized in Figures 1 and 3–5. These data, together with our earlier results, yield answers to a number of questions concerning ligand binding in heme proteins:

Decomposition of $N(t)$ into Three Processes. The decomposition of $\Delta A(t)$ [=0.56 $N(t)$] into three processes as shown in Figure 5 is essential for the following discussion. The validity of the decomposition is consequently important. The solvent process S is easily distinguished and subtracted; it is nearly exponential in time, and the characteristic rate coefficient λ_{on} is proportional to the CO concentration in the solvent. The difference, $N(t) - N_S(t)$, can in principle be fit by a sum of exponentials at each temperature, but the number of exponentials required for a good fit is so large that no unambiguous decomposition with smooth temperature dependence is obtained. Figures 3 and 4 and many similar curves in other heme proteins (Austin et al., 1975; Alberding et al., 1978; Stetzkowski et al., 1985) suggest the presence of two processes, I and M, besides the solvent process. The break between I and M is seen clearly in Figures 3 and 4. The two are nonexponential in time below about 260 K and vary smoothly with temperature. We consequently decompose $N(t) - N_S(t)$ into the components I and M for temperatures above 180 K. We define $N_I(t)$ as the fraction of photodissociated ligands that contribute to process I and that have not yet rebound at a time t after photodissociation. The nonexponential process I can still be approximated to a power law so that $N_I(t)$ is given by

$$N_I(t) = N_I(1 + t/t_0)^{-n} \quad (7)$$

where N_I is the amplitude of process I. Below about 180 K $N_I = 1$ and $N(t) \equiv N_I(t)$. The amplitudes N_I, N_M, and N_S (the fractions of photodissociated proteins that rebind a ligand via process I, process M, and process S respectively; $N_I + N_M + N_S = 1$) are given in Figure 6 as functions of temperature. We interpret the three processes I, M, and S as rebinding after photodissociation from the pocket, the matrix (globin and/or hydration shell), and the solvent.

Validity of the Sequential Model. We have justified the use of a sequential model earlier (Austin et al., 1975), and we repeat and extend the arguments here. The three processes observed above 240 K, with differing temperature dependences, can be sequential or parallel. S must be in sequence with I

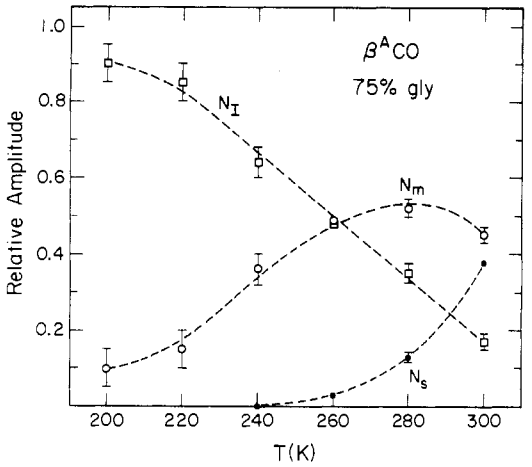

FIGURE 6: Relative amplitudes of process I (N_I), matrix process (N_M), and solvent process (N_S) for β^A CO in 75% glycerol–water.

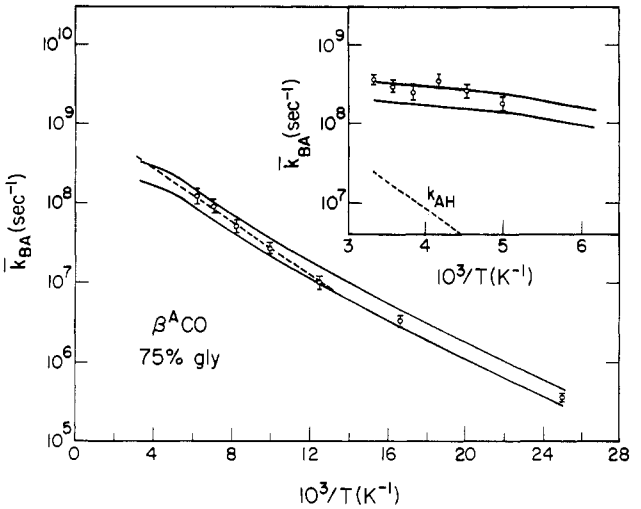

FIGURE 7: Plot of $\bar{k}_{BA}$ vs. $10^3/T$ for β^ACO in 75% glycerol–water. The solid lines are based on the model of Young and Bowne as described in the text, and the circles are given by eq 9. The dashed line is an empirical fit to the points given by eq 9. An expanded plot of $\bar{k}_{BA}$ vs. $10^3/T$ for high temperatures is shown in the insert. The circles are given by eq 9. k_{AH}, the rate coefficient for the relaxed process I, as predicted by Agmon and Hopfield, is shown in the insert as a dashed line.

and M because it corresponds to binding from the solvent. The simplest model, supported by theoretical arguments (Case & Karplus, 1979), then is the one given in eq 1, with all three processes in sequence. The most important ingredient of this model, the fact that the barrier B → A operates at all temperatures and is always the last step in binding, is supported by three experimental observations: (a) Process I can be seen up to 300 K in β^A (Figures 3 and 4) and β^{ZH} (Dlott et al., 1983). (b) The pH dependence of λ_{on} at about 300 K in Mb and in β^A is explained entirely by the pH dependence of $\bar{k}_{BA}$, measured at low temperatures and extrapolated to 300 K (Doster et al., 1982). (c) The pressure dependence of k_{BA} in the binding of CO to Mb has been measured at low temperatures (Sorensen, 1980) and at room temperature (Hasinoff, 1974; Caldin & Hasinoff, 1975). The reaction rate at all temperatures increases with pressure, and the activation volumes are approximately equal. This observation again implies that the innermost barrier B → A is still operative at room temperature. While schemes more complicated than eq 1 can also explain these observations, we have not found one that is as simple as the sequential barrier model. Since this model explains all data in the temperature range from 4 to 300 K and the time range from about 30 ps to ks, we consider assumptions i and ii to be verified.

Determination of $\bar{k}_{BA}$. The treatment of the binding at high temperatures, in particular the application of eq 5, requires the knowledge of $\bar{k}_{BA}$. We obtain $\bar{k}_{BA}$ above 180 K in two steps: We first determine $\bar{k}_{BA}(T)$ from 40 to 160 K and then extrapolate to temperatures above 180 K. Here we discuss the first step. We determine $\bar{k}_{BA}(T)$ from 40 to 160 K in two different ways: (a) We find empirical values for $\bar{k}_{BA}(T)$ by noting that, at time $t = 0$, immediately after photodissociation, all molecules are in well B and all contribute with equal weight to rebinding so that at all temperatures

$$\bar{k}_{BA} = -dN/dt \qquad (t = 0) \tag{8}$$

If data at very short times are available, eq 8 can be used directly. Since we do not yet have data of sufficient accuracy, we use the empirical fit eq 7. Below about 180 K $N(t) \equiv N_I(t)$ and eq 7 and 8 together give

$$\bar{k}_{BA} = N_I n/t_0 \tag{9}$$

Below about 180 K, $N_I = 1$ and values of n and t_0 can be extracted directly from the measured $N(t)$. The resulting coefficients $\bar{k}_{BA}(T)$ are given in Figure 7. (b) We fit $N(t)$ at all temperatures between 40 and 160 K to the model of Young and Bowne, obtain the temperature-independent distribution $g(H_{BA})$ given in Figure 2, and compute $\bar{k}_{BA}(T)$ with eq 6. The result is shown as solid lines in Figure 7. The two lines correspond to two different fits; the upper line follows from a $g(H_{BA})$ that fits the lower temperatures (40–80 K) best, the lower one reproduces the higher temperatures (100 to 160 K) best. The two lines indicate the error involved in determining $g(H_{BA})$. The two methods yield values for $\bar{k}_{BA}$ that differ by less than a factor of 2. In the absence of good picosecond data, method b is more accurate because it incorporates all data into a single distribution.

Extrapolation of the Low-Temperature Data. We extrapolate $\bar{k}_{BA}$ to temperatures above 200 K in two different ways: (a) The values of $\bar{k}_{BA}(T)$ obtained with eq 9 can be extrapolated without a model. Because $\bar{k}_{BA}(T)$ is not expected to follow an Arrhenius relation over the entire temperature range (Austin et al., 1975), we use only the data above about 80 K with the result indicated as the dashed line in Figure 7. (b) The model of Young and Bowne predicts how $g(H_{BA})$ changes with temperature above about 200 K. Inserting the predicted $g(H_{BA},T)$ into eq 6 yields the two solid lines drawn in Figure 7 for the two different fits described. The difference between methods a and b is less than a factor of 2.

To test the extrapolation, we determine the average rate coefficient $\bar{k}_{BA}$ above 180 K by using eq 8 which is valid at all temperatures. In the limit $k_{MB} \ll k_{BM}$ the slope dN/dt ($t = 0$) is approximately equal to the slope dN_I/dt ($t = 0$), and eq 9 still follows from eq 7 and 8. Since processes I and M are well separated in time, the above inequality is a reasonable assumption. We therefore fit eq 7 to the subtracted nonexponential process I and use eq 9 to obtain $\bar{k}_{BA}$. Above 260 K in 75% glycerol–water solution, process I is approximately exponential, $N_I(t) = N_I \exp(-t/t_0)$. Equation 8 then gives $\bar{k}_{BA} = N_I/t_0$. The experimentally determined values of $\bar{k}_{BA}$ are plotted in the insert in Figure 7. The agreement between the extrapolated and the measured rates is very good. The experiment consequently verifies assumption iii for β^A.

The characteristic rate coefficient for process I, $\bar{\lambda}_I$, can be defined as

$$\bar{\lambda}_I = \frac{-1}{N_I}\frac{dN_I}{dt}(t = 0) \tag{10}$$

Table I: Parameter for Binding of CO to Four Heme Proteins in 75% Glycerol–Water[a]

	low-temperature data		data at 300 K					
system	H_{BA}^{peak} (kJ/mol)	log A_{BA} (s^{-1})	G_{BA} (kJ/mol)	$-TS_{BA}$ (kJ/mol)	$\bar{k}_{BA}$ ($\times 10^6$ s^{-1})	λ_{on} ($\times 10^3$ s^{-1})	N_S	P_B ($\times 10^{-6}$)
β^ACO	3.6	9.5	24	20	330	4.6	0.38	40
MbCO	10.7	9.1	35	24	8	0.5	≈1	60
β^{ZH}CO	2.3	9.2	22	20	1700	23	0.5	30
LbCO	6.7	9.6	28	21	120	6.8	0.84	70

[a] $-TS_{BA}$ is the entropic contribution to the barrier at the heme.

Equation 10 together with eq 7 gives $\bar{\lambda}_I = n/t_0$. Therefore, in the limit $k_{MB} \ll k_{BM}$

$$\bar{\lambda}_I = \bar{k}_{BA}/N_I \quad (11)$$

When the amplitude of process I is less than 1, the characteristic rate coefficient for process I is larger than the average rate coefficient for the step B → A. Although this increase may seem counterintuitive, eq 11 can be alternatively obtained with eq 1. Above 180 K the CO molecule has a finite probability of moving into the matrix (Figure 6). In the limit $k_{MB} \ll k_{BM}$, $\bar{\lambda}_I$ is equal to the characteristic rate coefficient for depletion of well B. The opening of a second reaction channel, viz., B → M, increases the rate coefficient for depletion of well B, which is now given by the sum of the individual rate coefficients. Therefore

$$\bar{\lambda}_I = \bar{k}_{BA} + \bar{k}_{BM} \quad (12)$$

In the simplest model the ratio $\bar{k}_{BA}/\bar{k}_{BM}$ is equal to the fraction of proteins that recombine via process I to that which recombine via process M and S:

$$\bar{k}_{BA}/\bar{k}_{BM} = N_I/(N_M + N_S) = N_I/(1 - N_I) \quad (13)$$

The characteristic rate coefficient $\bar{\lambda}_I$ then becomes

$$\bar{\lambda}_I = \bar{k}_{BA}[1 + (1 - N_I)/N_I] = \bar{k}_{BA}/N_I \quad (14)$$

and we regain eq 11.

Agmon and Hopfield have introduced a model in which the average barrier between wells B and A increases as the protein relaxes (Agmon & Hopfield, 1983b). Their model predicts for β^A an activation energy of 13.8 kJ/mol and a preexponential factor of 6×10^9 s^{-1} after relaxation. The corresponding rate coefficient k_{AH}, shown in the insert of Figure 7, is too slow to fit process I and too fast to characterize process M (Figure 3). Moreover, the observed processes I and M are nonexponential in time below about 280 K, whereas Agmon and Hopfield have a unique k_{AH}, indicating that the relaxed process is exponential. The model of Agmon and Hopfield does not describe CO binding to β^A.

We can now also discuss the question raised by Henry et al. (1983) quoted in the introduction. Henry et al. studied the binding of CO to Mb at room temperature and saw a process with an amplitude $a = 0.037$ and a rate coefficient $k_{gem} = 5.6 \times 10^6$ s^{-1}. They discussed two different models, one essentially the one given in our eq 1 and the other one with only two barriers. In the latter model k_{gem} characterizes direct binding to the heme and consequently would correspond to our $\bar{\lambda}_I$. With eq 11 the relevant rate coefficient $\bar{k}_{BA}$ would then become $\bar{k}_{BA}$ (293 K) = $ak_{gem} = 2.1 \times 10^5$ s^{-1}, about 40 times slower than the extrapolation of the low-temperature MbCO data (Table I). With eq 5, this value implies that $P_B(T)$ would be about 40 times larger than in our model (Doster et al., 1982). Assuming that the ligand is not bound in the pocket (Alben et al., 1982), $P_B(T)$ is a measure of the volume V_B from which the last binding step occurs. Since our model implies a pocket volume $V_B = 20$ Å^3, the two-barrier model would imply 800 Å^3 for V_B, much larger than found by X-ray diffraction. A second argument indicates that the two-barrier model leads to an unlikely value of the enthalpy barrier between B and A. As shown previously, the two-barrier model implies a value $\bar{k}_{BA} = 2.1 \times 10^5$ s^{-1} at room temperature. Assuming an Arrhenius relation and $A_{BA} = 10^9$ s^{-1}, this value gives an activation enthalpy $H_{BA} = 21$ kJ/mol. Such a high value is in disagreement with the temperature dependence of the association rate at room temperature (Austin et al., 1975). Considering all the evidence together we conclude that in β^A and Mb the model eq 1 describes the observed phenomena well and that the low-temperature data can be extrapolated to room temperature. In this model, the process observed by Henry et al. and characterized by k_{gem} describes the matrix process.

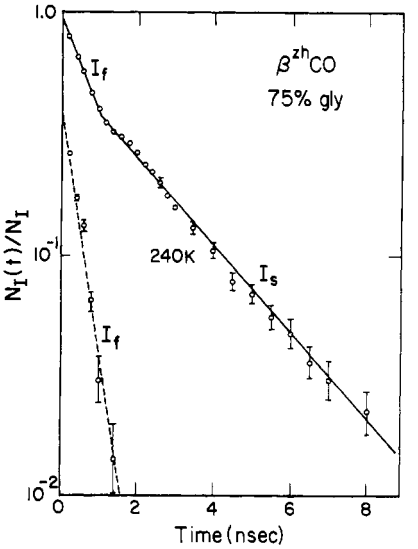

FIGURE 8: Semilogarithmic plot of CO binding to β^{ZH} at 240 K in 75% glycerol–water. The matrix and solvent processes have been subtracted from the recombination kinetics. The resultant process I has been scaled by its amplitude N_I. Process I shows two components, I_f and I_s. The dashed line is the fast component at 240 K after subtracting out I_s.

β^{ZH} Revisited. The agreement between the extrapolated and the observed values for the rate of process I at high temperatures for β^A raises the question as to why the same procedure appears to fail in β^{ZH}. To answer the question, we extended the binding data for β^{ZH} to shorter times. The data in Figure 8 show that process I at 240 K is biphasic. The fast component I_f is in the time range expected by extrapolation of process I from low temperature while the slow component I_s, already discussed in our earlier paper (Dlott et al., 1983), is significantly slower. Low-temperature recombination data for β^{ZH} CO in two different solvents (Figure 9) show a strong solvent dependence; process I is much faster in 60% EGOH–water than in the 99% glycerol–water solvent. Leghemoglobin also has an open pocket, and the solvent affects ligand binding at low temperatures (Stetzkowski et al., 1985). Observation of the CO stretching frequency with the FTIR technique described earlier (Alben et al., 1982) also indicates more

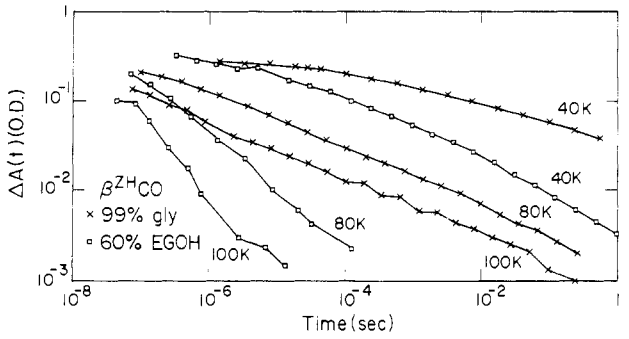

FIGURE 9: Recombination of CO with β^{ZH} in two different solvents, both buffered with phosphate to pH 7 at 300 K: 99% glycerol–water; 60% ethylene glycol–water.

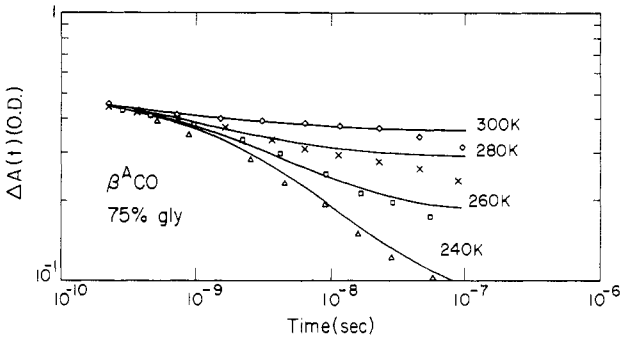

FIGURE 10: Expanded plot of the data in Figure 3. The solid lines are a fit to the data by using eq 15. The deviation at long times is a result of the recombination from the matrix which has not been incorporated in eq 15.

complexity in β^{ZH} than in β^{A}. The normal β chain shows only one band at 1951 cm^{-1}; in β^{ZH} a new band at 1970 cm^{-1} appears above 250 K in addition to the main band at 1959 cm^{-1}. With increasing temperature the new band increases at the expense of the main one. Room temperature IR spectroscopy measurements on carbonyl-Hb^{ZH} tetramer also show two bands at 1950.5 and 1958 cm^{-1}, in contrast with the single peak at 1951 cm^{-1} observed in carbonyl-Hb^{A} (Caughey et al., 1978). These observations are most likely connected with the presence of solvent in the pocket and with a large conformational change on deligation (Tucker et al., 1978; Phillips et al., 1981). The existing data are not sufficient to decide if the slow component of process I is due to the solvent in the pocket or conformation relaxation (Agmon & Hopfield, 1983a,b).

Time Dependence of $\bar{k}_{BA}$. Equations 5 and 6 together are valid if $\bar{k}_{BA}(T)$ at fixed T is independent of time after photodissociation. In the case of hemoglobin, Eaton and coworkers have pointed out that conformational relaxation may produce a time-dependent rate coefficient for ligand binding (Henry et al., 1984; Hofrichter et al., 1985). Friedman, Rousseau, and collaborators have studied the behavior of Raman bands in Hb and Mb (Friedman et al., 1982a–c; Friedman, 1985). They find that $\bar{k}_{BA}$ increases with $\nu_{Fe\text{-}His}$, the iron–histidine stretching frequency near 230 cm^{-1} observed in the deoxy species. Moreover, they show that in most heme proteins $\nu^{*}_{Fe\text{-}His}$, the stretching frequency observed 10 ns after photodissociation, is larger than $\nu_{Fe\text{-}His}$. Near 300 K $\nu^{*}_{Fe\text{-}His}$ evolves toward $\nu_{Fe\text{-}His}$ in microseconds to milliseconds. Taken together, these observations imply that $\bar{k}_{BA}(T)$ may not be time independent but may decrease with time after photodissociation as predicted by Agmon and Hopfield (1983). The effect is small for Mb and the monomeric β^{A}: In Mb, $\nu_{Fe\text{-}His}$ and $\nu^{*}_{Fe\text{-}His}$ are essentially identical. Within a few nanoseconds, the Soret peak in photodissociated β^{A} and deoxy-β^{A} (Lindqvist et al., 1980) and in photodissociated Mb and deoxy-Mb (Henry et al., 1983) are nearly identical, while they differ considerably in the tetrameric photodissociated Hb* and Hb. Support for a nearly time-independent $\bar{k}_{BA}$ in β^{A} comes also from the data in Table I. The values of P_B in Table I are calculated with $\bar{k}_{BA}$ assumed to be only a function of T, but not t. The resulting values of P_B, 60 × 10^{-6} for Mb and 40 × 10^{-6} for β^{A}, imply similar effective pocket volumes for Mb and β^{A}, in agreement with X-ray data. If $\bar{k}_{BA}$ in β^{A} were to decrease drastically after photodissociation, the observed λ_{on} would predict a much larger pocket volume for β^{A} than for Mb. The extrapolation procedure used in the present paper is consequently justified for the cases of Mb and β^{A}. The situation may be different in tetrameric cooperative hemoglobin where a time-dependent $\bar{k}_{BA}$ could be important for the function (Friedman, 1985).

Conformational Relaxation. We assume that the average conformational relaxation rate $\bar{\lambda}_r$ is faster than the solvent process rate λ_{on}, on the ground that the solvent process is observed to be exponential within experimental error. We can explicitly verify this assumption in β^{A}: the data indicate that process I in 75% glycerol–water is nonexponential in time at 260 K but is close to an exponential at 280 K. This observation implies that, in 75% glycerol–water, the relaxation rate coefficient $\bar{\lambda}_r$ is of the order of 10^{8} s^{-1} at 280 K. Since $\lambda_{on} \approx 10^{3}$ s^{-1} at 280 K, assumption iv, $\bar{\lambda}_r \gg \lambda_{on}$, is satisfied.

Influence of Protein Motion. We have stated earlier that the ligand could not move through the protein matrix if the matrix were rigid. The protein must fluctuate in order for the matrix and the solvent processes to take place. The migration through the globin should not be pictured as motion of the ligand in a fixed potential but a dynamic process in which the potential itself changes randomly in time. The activation energy for the motion B → M is consequently not expected to be unique but should be given by a distribution. This idea can be tested by a simulation of $N(t)$.

A complete treatment of the motion of the ligand is difficult. We only fit the data up to a time $t' = 1/k_{MB}$, where k_{MB} is the rate coefficient for return to the pocket from the matrix. We neglect return from the matrix so that our model eq 1 reduces to

$$\mathrm{M} \xleftarrow{k_{BM}} \mathrm{B} \xrightarrow{k_{BA}} \mathrm{A} \qquad (15)$$

The barrier H_{BA} is distributed as shown in Figure 2. If we assume a unique value for H_{BM}, we cannot fit the data. For simplicity we assume the barrier H_{BM} to be correlated with H_{BA} so that eq 13 holds. The barrier height distribution $g'(H_{BM})$ then has the same shape as $g(H_{BA})$. This assumption is not without justification because both barriers involve motion of the residues around and near the pocket, and a particular conformation of the protein may allow for more flexibility at the pocket than another. The important point, however, is that correlated distribution is the simplest assumption that does not involve additional parameters. More complicated models will fit the data if this simple one does. With this model the data can be fit well as shown in Figure 10. The fit corresponds to a preexponential $A_{BM} = 5 \times 10^{13}$ s^{-1}, and H^{peak}_{BM} [the barrier height for which $g'(H_{BM})$ has a maximum value] = 25 kJ/mol.

Control at the Heme. Relevant data for the binding of CO to four heme proteins are collected in Table I. H^{peak}_{BA} and A_{BA} are measured at low temperatures. The Gibbs activation energy $G_{BA} = H^{peak}_{BA} - TS_{BA}$ and the rate coefficient $\bar{k}_{BA}$ are obtained by extrapolation of the low-temperature data to 300 K. To calculate G_{BA}, we assume an "attempt frequency" of 10^{13} s^{-1}. For β^{A} the experimentally determined and the ex-

trapolated values of $\bar{k}_{BA}$ agree.

The Gibbs energy barrier at the heme is large because of a large entropic contribution. The entropic component, however, varies little among the four systems. The variable contribution comes from the small enthalpic component. This component, in turn, is most likely dominated by the proximal side of the heme (Doster et al., 1982).

Comparative investigations on the kinetics of the reaction of various monomeric heme proteins with isocyanides (DiIorio, Winterhalter, Anderluzzi, and Giacometti, unpublished observations) also show that the equilibrium distribution of the ligand between the solvent and the heme pocket, characterized by P_B, is not significantly influenced by changes in the primary structure of the protein as long as major changes in the heme pocket geometry are excluded.

We return to eq 5, $\lambda_{on} = \bar{k}_{BA} P_B N_S$, and the data in Table I to discuss the regulation of the physiologically significant association rate λ_{on}. The coefficient $\bar{k}_{BA}$ describes the rate of covalent bond formation between the heme iron and the ligand and is determined by the properties of the heme group and its surrounding (Doster et al., 1982; Friedman, 1985). P_B and N_S are determined by the overall protein structure. Table I shows that the product $P_B N_S$ varies by a factor of 4 for the heme proteins listed, whereas $\bar{k}_{BA}$ changes by over a factor of 200: Regulation of the association process is dominated by the covalent binding step at the heme. This step, in turn, is mainly determined by the barrier height H_{BA}. In order to understand the structure–function relationship, it is consequently necessary to study the dependence of H_{BA} and also A_{BA} on protein structure. Such studies are most efficiently performed at low temperatures where the step B → A can be explored directly. While in principle some of the information could also be obtained near room temperature, such studies yield at best $\bar{k}_{BA}$ and do not provide information about the enthalpy distribution $g(H_{BA})$, the fingerprint of each protein–ligand system.

Many of the results of the present and earlier work can only be obtained from data extending over wide ranges in temperature and time. The existence of at least three separate and distinct processes, I, M, and S, is not obvious from data taken only at room temperature. On cooling we see the distinct processes clearly. The temperature and time dependence of these processes permits the construction of the sequential-barrier model. Diffusion in the solvent is not rate limiting; the main regulation is at the heme during the covalent binding step. This crucial step can be characterized in great detail at low temperatures. At least in the monomeric heme proteins studied, the low-temperature rate can be extrapolated to room temperature. A consistent model for the binding of small ligands to heme proteins is the final result of these experiments.

ACKNOWLEDGMENTS

We thank Robert D. Young and Samuel F. Bowne for valuable discussions and advice.

Registry No. Hb^A, 9034-51-9; Hb^{ZH}, 9035-33-0; CO, 630-08-0.

REFERENCES

Agmon, N., & Hopfield, J. J. (1983a) *J. Chem. Phys. 78*, 6947–6959.

Agmon, N., & Hopfield, J. J. (1983b) *J. Chem. Phys. 79*, 2042–2053.

Alben, J. O., Beece, D., Bowne, S. F., Doster, W., Eisenstein, L., Frauenfelder, H., Good, D., McDonald, J. D., Marden, M. C., Moh, P. P., Reinisch, L., Reynolds, A. H., Shyamsunder, E., & Yue, K. T. (1982) *Proc. Natl. Acad. Sci. U.S.A. 79*, 3744–3748.

Alberding, N., Chan, S. S., Eisenstein, L., Frauenfelder, H., Good, D., Gunsalus, I. C., Nordlund, T. M., Perutz, M. F., Reynolds, A. H., & Sorensen, L. B. (1978) *Biochemistry 17*, 43–51.

Alpert, B., El Mohsni, S., Lindqvist, L., & Tfibel, F. (1979) *Chem. Phys. Lett. 64*, 11–16.

Ansari, A., Berendzen, J., Bowne, S. F., Frauenfelder, H., Iben, I. E. T., Sauke, T. B., Shyamsunder, E., & Young, R. D. (1985) *Proc. Natl. Acad. Sci. U.S.A. 82*, 5000–5004.

Antonini, E., & Brunori, M. (1971) *Hemoglobin and Myoglobin in Their Reactions with Ligands*, North-Holland, Amsterdam.

Austin, R. H., Beeson, K. W., Eisenstein, L., Frauenfelder, H., & Gunsalus, I. C. (1975) *Biochemistry 14*, 5355–5373.

Beece, D., Eisenstein, L., Frauenfelder, H., Good, D., Marden, M. C., Reinisch, L., Reynolds, A. H., Sorensen, L. B., & Yue, K. T. (1980) *Biochemistry 19*, 5147–5157.

Caldin, E. F., & Hasinoff, B. B. (1975) *J. Chem. Soc., Faraday Trans. 1 71*, 515–527.

Case, D. A., & Karplus, M. (1979) *J. Mol. Biol. 132*, 343–368.

Caughey, W. S., Houtchens, R. A., Lanir, A., Maxwell, J. C., & Charache, S. (1978) in *Biochemical and Clinical Aspects of Hemoglobin Abnormalities* (Caughey, W. D., Ed.) pp 29–56, Academic, New York.

Chernoff, D. A., Hochstrasser, R. M., & Steele, A. W. (1980) *Proc. Natl. Acad. Sci. U.S.A. 77*, 5606–5610.

Dlott, D. D., Frauenfelder, H., Langer, P., Roder, H., & Di Iorio, E. E. (1983) *Proc. Natl. Acad. Sci. U.S.A. 80*, 6239–6243.

Doster, W., Beece, D., Bowne, S. F., DiIorio, E. E., Eisenstein, L., Frauenfelder, H., Reinisch, L., Shyamsunder, E., Winterhalter, K. H., & Yue, K. T. (1982) *Biochemistry 21*, 4831–4839.

Dudell, D. A., Morris, R. J., & Richards, J. T. (1979) *J. Chem. Soc., Chem. Commun.* 75–76.

Dudell, D. A., Morris, R. J., Muttucumaru, N. J., & Richards, J. T. (1980) *Photochem. Photobiol. 31*, 479–484.

Frauenfelder, H. (1985) in *Structure and Motion: Membranes, Nucleic Acids and Proteins* (Clementi, E., Corongiu, G., Sarma, M. H., & Sarma, R. H., Eds.) pp 205–218, Adenine, Guilderland, NY.

Friedman, J. M. (1985) *Science (Washington, D.C.) 228*, 1273–1280.

Friedman, J. M., & Lyons, K. B. (1980) *Nature (London) 284*, 570–572.

Friedman, J. M., Stepnoski, R. A., Stavola, M., Ondrias, M. R., & Cone, R. L. (1982a) *Biochemistry 21*, 2022–2028.

Friedman, J. M., Rousseau, D. L., Ondrias, M. R., & Stepnoski, R. A. (1982b) *Science (Washington, D.C.) 218*, 1244–1246.

Friedman, J. M., Rousseau, D. L., & Ondrias, M. R. (1982c) *Annu. Rev. Phys. Chem. 33*, 471–491.

Giacometti, G. M., Brunori, M., Antonini, E., Di Iorio, E. E., & Winterhalter, K. H. (1980) *J. Biol. Chem. 225*, 6160–6165.

Gibson, Q. H. (1956) *J. Physiol. 134*, 112–122.

Hänggi, P. (1978) *J. Theor. Biol. 74*, 337–359.

Hasinoff, B. B. (1974) *Biochemistry 13*, 3111–3117.

Henry, E. R., Sommer, J. H., Hofrichter, J., & Eaton, W. A. (1983) *J. Mol. Biol. 166*, 443–451.

Henry, E. R., Hofrichter, J., Sommer, J. H., & Eaton, W. A. (1984) in *Brussels Hemoglobin Symposium 1983* (Schnek,

A. G., & Paul, C., Eds.) pp 193–203, Editions de l'Universite de Bruxelles, Bruxelles.
Hofrichter, J., Henry, E. R., Sommer, J. H., Deutsch, R., Ikeda-Saito, M., Yonetani, T., & Eaton, W. A. (1985) *Biochemistry 24*, 2667–2679.
Lindqvist, L., El Mohsni, S., Tfibel, F., & Alpert, B. (1980) *Nature (London) 288*, 729–730.
Lindqvist, L., El Mohsni, S., Tfibel, F., Alpert, B., & Andre, J. C. (1981) *Chem. Phys. Lett. 79*, 525–528.
Perutz, M. F., & Matthews, F. S. (1966) *J. Mol. Biol. 21*, 199–202.
Phillips, S. E. V., Hall, D., & Perutz, M. F. (1981) *J. Mol. Biol. 150*, 137–141.
Sorensen, L. B. (1980) *Dissertation*, University of Illinois—Urbana, Champaign, IL.
Stetzkowski, F., Banerjee, R., Marden, M. C., Beece, D. K., Bowne, S. F., Doster, W., Eisenstein, L., Frauenfelder, H., Reinisch, L., Shyamsunder, E., & Jung, C. (1985) *J. Biol. Chem. 260*, 8803–8809.
Tucker, P. W., Philips, S. E. V., Perutz, M. F., Houtchens, R., & Caughey, W. S. (1978) *Proc. Natl. Acad. Sci. U.S.A. 75*, 1076–1080.
Young, R. D. (1984) *J. Chem. Phys. 80*, 554–560.
Young, R. D., & Bowne, S. F. (1984) *J. Chem. Phys. 81*, 3730–3737.

Human von Willebrand Factor: A Multivalent Protein Composed of Identical Subunits†

Michael W. Chopek,* Jean-Pierre Girma,‡ Kazuo Fujikawa, Earl W. Davie, and Koiti Titani
Department of Biochemistry, University of Washington, Seattle, Washington 98195
Received August 27, 1985; Revised Manuscript Received March 4, 1986

ABSTRACT: A large-scale method for the isolation of von Willebrand factor (vWF) from human factor VIII concentrates was developed in order to study the structure of this protein and its platelet binding activity. vWF is composed of a number of glycoprotein subunits that are linked together by disulfide bonds to form a series of multimers. These multimers appear to contain an even number of subunits of 270K. Two minor components of M_r 140K and 120K were also identified, but these chains appear to result from minor proteolysis. The smallest multimer of vWF contained nearly equimolar amounts of the 270K, 140K, and 120K subunits, while the largest multimers contained less than 20% of the two minor components. Amino acid sequence analysis, amino acid composition, and cleavage by cyanogen bromide indicate that the 270K subunits are identical and each is a single polypeptide chain with an amino-terminal sequence of Ser-Leu-Ser-Cys-Arg-Pro-Pro-Met-Val-Lys and a carboxyl-terminal sequence of Glu-Cys-Lys-Cys-Ser-Pro-Arg-Lys-Cys-Ser-Lys. Platelet binding in the presence of ristocetin was 8-fold greater with multimers larger than five (i.e., containing more than 10 subunits of 270K) as compared to multimers less than three (containing less than six subunits of 270K). However, partially reduced vWF (M_r 500K), regardless of whether it was prepared from large or small molecular weight multimers, gave platelet binding similar to that of the smallest multimers. Likewise, partial proteolysis by elastase, thermolysin, trypsin, or chymotrypsin produced small "multimer-like" proteins with platelet binding properties similar to either partially reduced vWF or to the smallest multimers. We conclude that human vWF contains identical 270K subunits assembled into a multivalent structure. Disassembly by either partial reduction or partial proteolysis produces essentially monovalent protein with platelet binding properties similar to that of the smallest multimers. Multivalency is likely the primary factor responsible for the increase in biological activity with multimer size.

Human von Willebrand factor (vWF)[1] is a large glycoprotein that circulates in plasma as a series of subunits or multimers linked by disulfide bonds. A very small amount of vWF is also complexed with factor VIII, a trace protein absent or modified in hemophilia A (Hoyer, 1981). vWF is also involved in platelet adhesion to subendothelium, leading to the formation of the platelet plug during vascular damage (Tschopp et al., 1974; Meyer & Baumgartner, 1983). Accordingly, individuals lacking vWF may have low factor VIII coagulant activity resulting in impaired fibrin formation as well as prolonged bleeding time due to poor platelet plug formation. Biological activity of human vWF is measured in vitro by its ability to promote platelet aggregation or to bind to specific receptors on the platelet membrane (Kao et al., 1979). Both measurements require the presence of a cofactor, such as ristocetin (Harrison & McKee, 1983). Thrombin,

† This work was supported in part by National Institutes of Health Grant HL 16919 to E.W.D., Grant HL 29595 to K.T., and Training Grant T32 HL 07150. M.W.C. was the recipient of Individual Postdoctoral Fellowship HL 06281. J.-P.G. was the recipient of a Bourse d'étude des Laboratoires Anphar-Rolland and Grants from the Philippe Foundation, Inc., and NATO.
* Address correspondence to this author at St. Paul Regional Red Cross, St. Paul, MN 55107, or Department of Laboratory Medicine and Pathology, University of Minnesota, Minneapolis, MN 55455.
‡ Present address: INSERM U.143, Hôpital de Bicêtre, 94270 Le Kremlin-Bicêtre, France.

[1] Abbreviations: vWF, von Willebrand factor; $NaDodSO_4$, sodium dodecyl sulfate; Tris, tris(hydroxymethyl)aminomethane; EDTA, ethylenediaminetetraacetic acid; V_e/V_t, elution volume at the protein peak (V_e) divided by the total volume of packed column bed (V_t).

0006-2960/86/0425-3146$01.50/0